ChemPubSoc Europe

DOI: 10.1002/cphc.201402820

CHEMPHYSCHEM Articles

Effect of Nitrogen and Fluorine Co-substitution on the Structure and Magnetic Properties of Cr_2O_3

Jaysree Pan,[b] Umesh V. Waghmare,[b] Nitesh Kumar,[a] C. O. Ehi-Eromosele,[a] and C. N. R. Rao*[a]

First-principles density functional calculations were carried out to determine the structure as well as electronic and magnetic properties of N and F co-substituted Cr_2O_3. The formation of strong Cr–N bonds upon substitution of oxygen with nitrogen leads to large distortions in the local structure and changes in magnetic moments, which are partly compensated by co-substitution with fluorine. The effects of spin–orbit coupling are relatively weak, but its combination with local structural distortions gives rise to canting of spins and an overall magnetic moment in N, F co-substituted Cr_2O_3. Experimentally, we observe spin canting in N, F co-substituted Cr_2O_3 with considerable enhancement in the coercive field at low temperatures.

1. Introduction

It is customary to substitute the cation in metal oxides to change the structure and properties. However, substituting the oxide ion with other anions would be expected to have more significant effects on the electronic structure and properties. There have been a few studies of nitrogen substitution in place of oxygen in TiO_2, and such substitution changes the electronic properties significantly, rendering the material somewhat colored. Nitrogen substitution in the oxygen site has a major disadvantage, as this creates oxygen vacancies. Furthermore, such oxygen vacancies give rise to ferromagnetic interactions.[1,2] It would, therefore, be necessary to carry out co-substitution of oxygen by nitrogen and fluorine to avoid the creation of vacancies and other defects. Co-substitution of N and F in ZnO and TiO_2 has indeed been studied.[3,4] These studies have shown that the oxides become colored with corresponding changes in the UV/Vis spectra and an associated decrease in the band gap. Thus, N, F co-substituted ZnO is orange in color with a much smaller band gap than the parent oxide. There has been no study on the effect of such co-substitution of N and F on the magnetic properties of oxides. Cr_2O_3 is a linear magnetoelectric material, in which a magnetic field can proportionally induce electrical polarization.[5] Above room temperature, the antiferromagnetic transition temperature (ca. 307 K) in Cr_2O_3 makes it more important for future applications for example in spintronics.[6] It is, therefore, interesting to examine the effect of co-substitution of N and F on the magnetic properties of antiferromagnetic Cr_2O_3. Herein, we discuss the results of our detailed first-principles calculations on the substitution of N and F in Cr_2O_3. We also present the results of our experimental study into the magnetic properties of Cr_2O_3 substituted by both N and F. We compare the results of the effect of co-substitution of N and F with those obtained with fluorine substitution alone.

[a] Dr. N. Kumar, C. O. Ehi-Eromosele, Prof. C. N. R. Rao
Chemistry and Physics of Materials Unit
New Chemistry Unit and International Centre for Materials Science
Jawaharlal Nehru Centre for Advanced Scientific Research
Jakkur P.O., Bangalore-560064 (India)
E-mail: cnrrao@jncasr.ac.in

[b] J. Pan, Prof. U. V. Waghmare
Theoretical Sciences Unit
Jawaharlal Nehru Centre for Advanced Scientific Research
Jakkur P.O., Bangalore-560064 (India)

2. Results and Discussion

2.1. Theory

The estimates of lattice parameters of Cr_2O_3 obtained from DFT calculations agree well with experimental findings[7–12] and earlier DFT-based studies[13–15] (Table 1). Each oxygen atom is bonded to three nearest neighbors through octahedrally coordinated Cr atoms with bond lengths of 1.96, 1.96, and 2.00 Å. Our self-consistent and fully relaxed calculations give the magnetic ground state of pristine Cr_2O_3 with $+-+-+-$ antiferromagnetic ordering of spins at Cr sites along the *c* direction (Figure 1a) of the hexagonal cell, which is in agreement with the stable magnetic state found experimentally up to the Neél temperature of 307 K.[13,14] The partial density of states of pristine Cr_2O_3 in Figure 2a reveals that the highest energy valence band is primarily contributed by Cr 3d (t_{2g}) states, with a sizeable component of O 2p orbitals, indicating a strong hybridization between d orbitals of Cr and p orbitals of O. Such an electronic structure with three majority spin electrons in the 3d orbitals of Cr^{3+} gives a local magnetic moment of 2.85 μ_B, which is close to the ideal value of 3 (hybridization between Cr 3d and O 2p orbital results in a slight reduction in the magnetic moment). The lowest energy conduction band is constituted of the e_g orbitals of Cr. Our estimate of the band gap (2.73 eV) is 20% lower than the experimental band gap of 3.4 eV, as typically expected of DFT calculations. We note that this gap is a result of a combination of crystal-field (ca. 3 eV) and

Table 1. Theoretical results of pure $Cr_{12}O_{18}$ and comparison with results of experiments and other calculations.

	Lattice Parameters						Δ_{gap}[a] [eV]	m_{Cr}[b] [μ_B]
	a [Å]	*b* [Å]	*c* [Å]	α [°]	β [°]	γ [°]		
Theory	4.94	4.94	13.56	90.00	90.00	120.00	2.73	2.85
Experiment	4.96	4.96	13.59	90.00	90.00	120.00	3.40	2.48/2.76
Theory[c]	5.07[d]	5.07[d]	13.84[d]	90.00[d]	90.00[d]	120.00[d]	2.60[d]	3.01[d]/2.86[e]

[a] Δ_{gap} = electronic band gap. [b] m_{Cr} = magnetic moment on Cr 3d orbital. [c] DFT calculations performed by other groups. [d] GGA + U (5 eV) calculation. [e] LDA + U (4 eV) calculation. Table 2
Structural parameters and electronic band gaps of pure and doped $Cr_{12}O_{18}$.

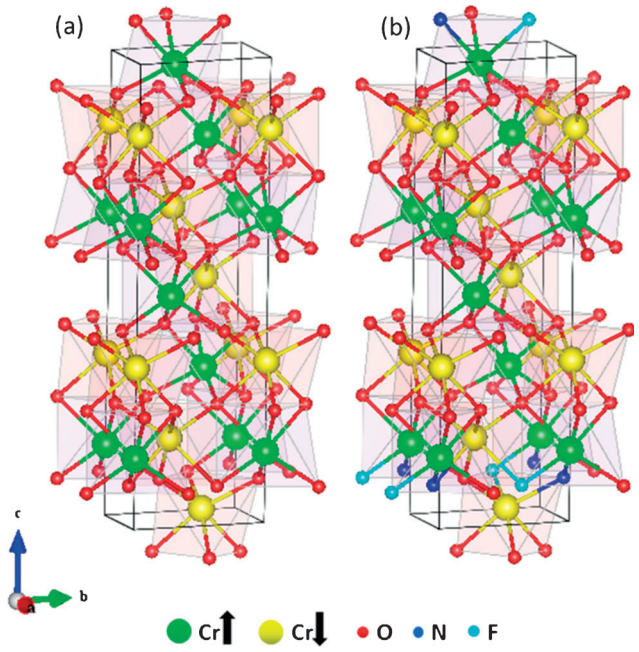

Figure 1. a) Hexagonal cell of undoped Cr_2O_3 with Cr having +−+−+− spins at neighbouring sites on the Cr–O–Cr chains along the *c* axis and b) phase-separated layered structure in energetically lowest configuration of N and F co-substituted Cr_2O_3.

a strong-exchange splitting (4.5 eV), and it separates the d bands of Cr.

The formation energies of substitution of nitrogen, fluorine, as well as both nitrogen and fluorine in Cr_2O_3 are 3.076, 1.071, and 3.775 eV, respectively, which means that co-substitution of N, F is favoured with respect to substitution of N or F alone. We first examine the effects of substitution of a single anionic species (F or N). Substitution of N at an O site results in the formation of two strong Cr–N bonds (1.84 and 1.87 Å) and one Cr–N bond (1.96 Å), which is comparable to the Cr–O bond length. This is accompanied by a small (< 1%) contraction of the lattice parameters. Owing to the deficiency of one electron per unit cell, it results in an overall magnetic moment of approximately 0.5 μ_B per formula unit. On the other hand, substitution of F at the O site results in the formation of slightly longer and weaker bonds of 1.97, 2.01, and 2.05 Å, and the lattice constants are almost unchanged (Table 2). This structural change is accompanied by an overall magnetic moment of about 0.15 μ_B per formula unit. It is, therefore, evident that local structural changes may influence the magnetic properties of Cr_2O_3 significantly, that is, leads to ferrimagnetism in Cr_2O_3.

We now turn to analysis of N, F co-substituted Cr_2O_3. Based on the site occupancy disorder (SOD) analysis of the hexagonal supercell of $Cr_{12}O_{16}NF$, ten symmetry-inequivalent configurations are possible (see Figure S1 a–j in the Supporting Information) for the replacement of two oxygen atoms with one N atom and one F atom. Carrying out the structural relaxation of each configuration, we evaluate their relative stability from the energetics (Table 3). The lowest energy configuration involves N and F atoms that are bonded to the same Cr atom, and the N, Cr, and F atoms make an angle of 97.6° (Figure 1 b). In all of the configurations, the N–Cr bond length is shorter by approximately 1–2% and the F–Cr bond length is longer by approximately 2–3.5% with respect to the O–Cr bond length in pristine Cr_2O_3. In the configuration that is second lowest in energy (6.7 meV per formula unit relative to the ground state, see Table 3), N and F are bonded to the same Cr atom. Formation of N–Cr–F bonds minimizes the overall structural distortion (strain) by trapping it locally to a single layer in the lowest energy configuration (Figure 1 b), in which both N and F atoms

Table 2. Structural parameters and electronic band gaps of pure and doped Cr_2O_3.

	Lattice Parameters						Δ_{gap} [eV]
	a [Å]	*b* [Å]	*c* [Å]	α [°]	β [°]	γ [°]	
$Cr_{12}O_{18}$	4.94	4.94	13.56	90.00	90.00	120.00	2.73
$Cr_{12}O_{17}N$	4.91	4.89	13.45	89.84	90.07	119.86	0.00
$Cr_{12}O_{17}F$	4.92	4.91	13.52	90.05	90.40	119.82	0.00
$Cr_{12}O_{17}$	4.89	4.89	13.43	90.36	89.64	119.98	0.00
$Cr_{12}O_{16}NF$	4.95	4.95	13.59	89.93	90.01	120.04	2.02

Table 3. Relative energies of various N, F co-substituted Cr_2O_3 ($Cr_{12}O_{16}NF$) configurations obtained from calculations with collinear magnetic ordering.

Configuration	ΔE[a] [meV]
a	0.00
b	40
c	317
d	40
e	329
f	339
g	324
h	395
i	423
j	395

[a] ΔE = relative total energy of the system ($Cr_{12}O_{16}NF$).

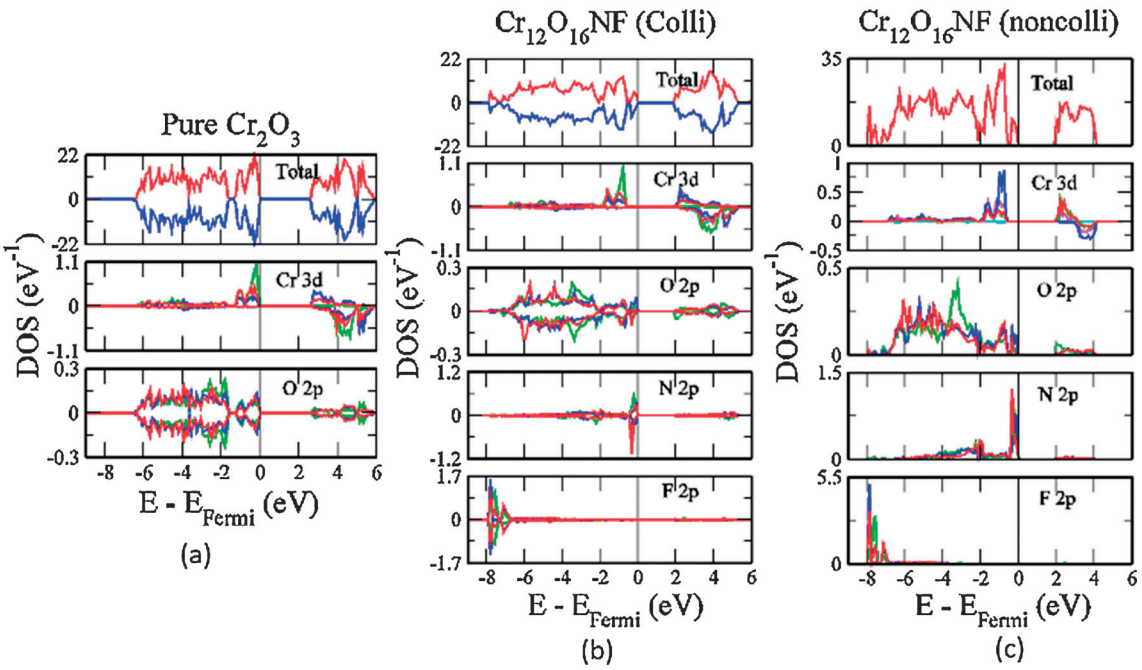

Figure 2. Electronic density of states of a) pure Cr_2O_3. Electronic density of states of N, F co-doped Cr_2O_3 obtained with calculations based on b) collinear (colli) and c) non-collinear (noncolli) magnetic ordering. O, N, and F 2p orbitals: red line is p_x, green line is p_y, and blue line is p_z. Cr 3d orbitals: cyan line is d_{xy}, magenta line is d_{yz}, blue line is d_{zx}, red line is d_{z^2} and green line is $d_{x^2-y^2}$.

occupy O sites in the (001) plane. Consequently, the volume of octahedral CrO_4NF increases by 1.6% compared to CrO_6 in pristine Cr_2O_3. From the lattice parameters of the relaxed structures (Table 3), we see that N, F co-substitution leaves the cell size almost unchanged (Figure 3). A similar structural change has been noted in $BaTiO_3$ co-substituted with N and F[16].

We found that the electronic band gap decreases to 2.02 eV with N and F co-substitution in Cr_2O_3 (Table 2). In the electronic density of states of co-substituted Cr_2O_3 ($Cr_{12}O_{16}NF$) (Figure 2b), the topmost valence band has a width of about 0.6 eV and largely consists of N 2p states, with some contribution from O 2p states. The latter reflects the superexchange interaction mediated through anionic p orbitals. The 3d states of Cr are approximately 0.7 eV lower in energy with respect to the valence band maximum of $Cr_{12}O_{16}NF$. It is clear that the reduction in the band gap by approximately 0.67 eV is cause by the sub-band of N 2p states that appear in the gap, and that the orbital character of the bands lining the gap is qualitatively different to that of pristine Cr_2O_3. Anionic F is relatively inert compared to O and N, because its 2p states are approximately 7 eV below the valence-band maximum; although it plays an important role in the structural stability, it seems to be silent in the electronic activity.

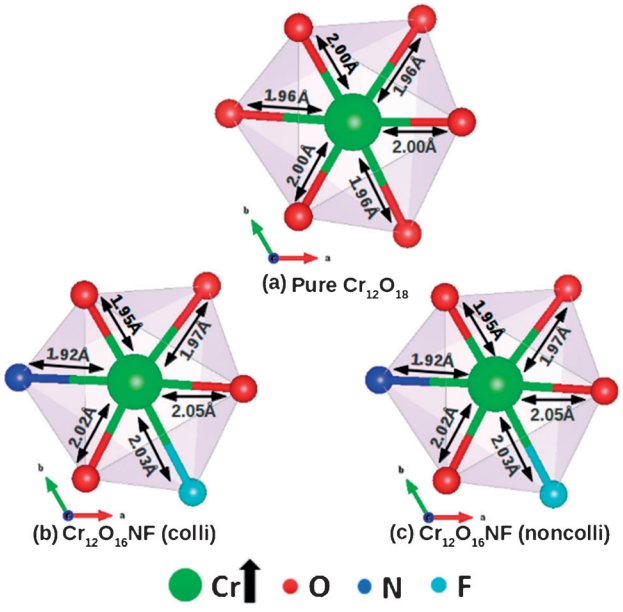

Figure 3. Structural changes owing to co-substitution of N and F in Cr_2O_3 with collinear (colli) and non-collinear (noncolli) calculations.

To study the non-collinearity in the magnetic ordering of anion-substituted Cr_2O_3, we optimized the structure and spin magnitudes along the *x*, *y*, and *z* axes, simultaneously, in an unbiased manner [fully unconstrained (FU) non-collinear method] for each of the Cr sites. Such a calculation with fully unconstrained non-collinear spins does *not* include spin–orbit coupling (SOC). It treats the magnetization as a continuous, spatially varying, vector field, and hence leads to relatively high symmetry during the optimization of the non-collinear magnetic moments.[17] As the local structural symmetry is broken at anion-substituted sites, we expect changes in the crystal-field-split d orbitals and we carried out another set of calculations (non-collinear SOC) that include the SOC to determine the effects of coupling between orbitals (spatial degrees of freedom) and magnetic spin.

The net magnetic moment of pristine Cr_2O_3 (see Table S1) is very small or almost zero, even after inclusion of the SOC, even though the spins do exhibit slight deviation from the antiparallel alignment (canting). The effects of N substitution, F substitution, O vacancies, and N, F co-substitution on the local magnetic moments in Cr_2O_3 are presented in Tables S2–S5. For N-substituted Cr_2O_3, we find a substantial net magnetic moment, but not all of it is attributed to canting. There is a large variation in the local magnetic moment of Cr ions from one site to another, which is expected from the significant deviation in the structure and hybridization between 2p orbitals of N and 3d orbitals of Cr. Owing to the partially occupied sub-band of the former at the valence-band maximum, a large part of the net magnetization arises from the hole-mediated interaction in N–Cr_2O_3. In addition, the effect of SOC is quite sizeable (see Table S2 and compare moments arising from FU and SOC calculations). This is unique to N substitution (we find much weaker effect of the SOC in F-substituted Cr_2O_3). This can be understood from the fact that the topmost valence band (N 2p sub-band) is strongly hybridized with the 3d states of Cr and is separated with a tiny gap (of 0.1 eV) from the Cr 3d bands. As a result, the perturbative effect of the SOC is enhanced. In contrast, the local moments do not change much, owing to SOC in F-substituted Cr_2O_3, because the 2p states of F are very low in energy. In $Cr_2O_{3-\delta}$, we do not see any significant net magnetization or any canting of spins. Thus, our calculations clearly confirm the canting of spins and, hence, an overall net magnetization caused by anionic substitution, and its primary cause in the local structural distortions associated with N substitution in Cr_2O_3.

For SOC-based calculation of N, F co-substituted Cr_2O_3, we start with the electronic and magnetic structure of the lowest energy configuration (Figure 1 b) obtained from our calculations with collinear magnetic ordering. We find that the SOC results in a significant enhancement in 1) the net magnetic moment and 2) canting. Owing to weaker local structural distortions and a fully occupied N 2p sub-band (and hence lack of hole-mediated interactions), the net magnetic moment here is much smaller than in N- or F-substituted Cr_2O_3. We note that the effect of SOC on electronic structure in the vicinity of the gap is rather weak. Thus, canting of spins arises primarily from the contribution of local structural distortions through the SOC.

Anion substitution leads to locally broken symmetry, marked by the displacement of atoms with respect to their positions in pristine Cr_2O_3 (Figure 4 b, Figure 4 c, and Figure 4 e). It should be clear from this picture that the hexagonal ring with a N atom at the center shrinks, whereas that with a F atom expands with respect to the unsubstituted layers, creating a local distortion of the structure. On the other hand, such structural distortions are negligible in Cr_2O_3 with an O vacancy (Figure 4 d). For anion-substituted Cr_2O_3, canting can be explained by using simple anti-symmetric exchange, arising from the interaction between spins at the two neighboring sites, also known as the Dzyaloshinskii–Moriya interaction[18] (Figure 5) originating from the SOC, which can be expressed by Equation (1):

$$\vec{H}_{AB} = \vec{D}_{AB} \cdot \left(\vec{S}_A \times \vec{S}_B\right) \quad (1)$$

where S_A and S_B are spins at the two neighboring sites A and B. D_{AB} depends on the coupling constant D_0 and structural geometry (Figure 5), as shown in Equation (2):

$$\vec{D}_{AB} \propto D_0\left(\Delta\vec{x} \times \vec{r}\right) \quad (2)$$

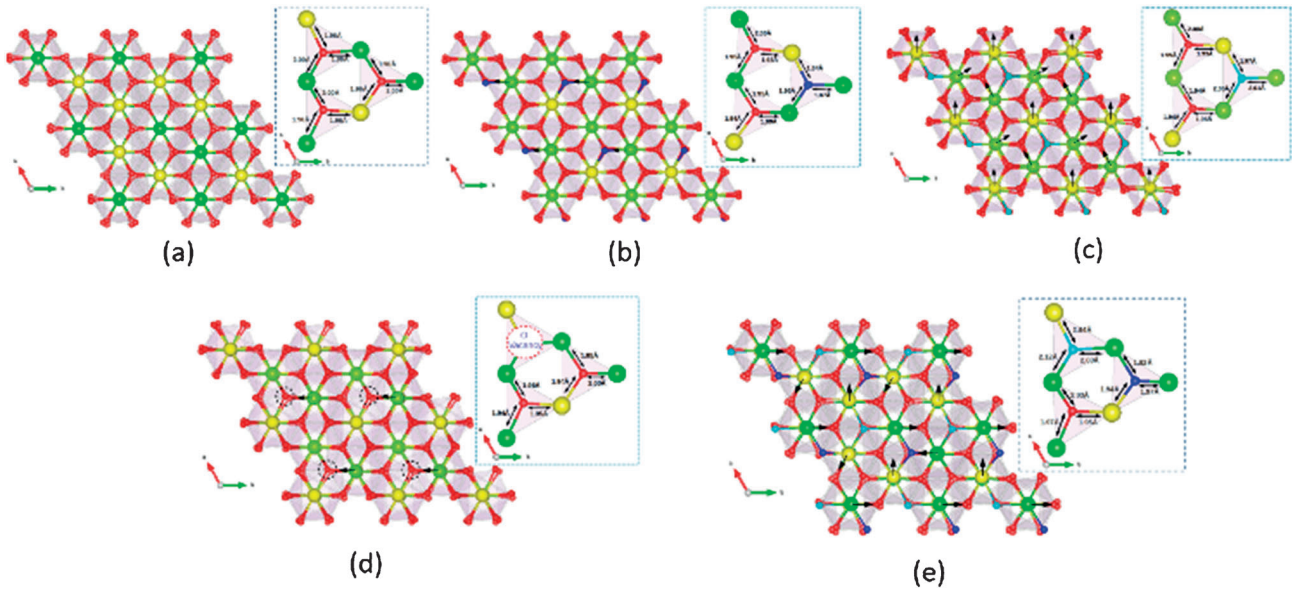

Figure 4. Frustrated lattice of Cr in (110) planes of a) pristine Cr_2O_3, b) N-doped Cr_2O_3, c) F-doped Cr_2O_3, d) Cr_2O_3 with an O vacancy, and e) N, F co-doped Cr_2O_3. Cr_2O_3. The relative movement of Cr ions in the doped layer compared to one layer below it (undoped layer) is schematically indicated by black arrows in the diagram.

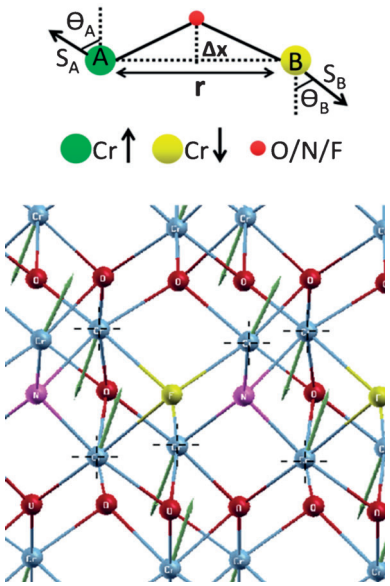

Figure 5. Schematic diagram of anti-symmetric exchange arising from local structural distortions in anion-substituted Cr_2O_3 (top) and lowest energy structure of N, F co-substituted Cr_2O_3 obtained from a calculation including spin–orbit coupling (bottom).

where $\vec{r}$ is the vector connecting site A and B and $\Delta\vec{x}$ is the perpendicular distance of the anion from the line AB. The Dzyaloshinskii–Moriya coupling is only nonzero if $\Delta\vec{x}$ is nonzero, that is, Cr_A–X–Cr_B is not linear. In addition, there should be deviation from the antiparallel (or parallel) alignment of S_A and S_B. In the case of pure Cr_2O_3, spins are exactly antiparallel and the Dzyaloshinskii–Moriya interaction vanishes. For the anion-substituted case, structural distortion breaks the symmetry locally and the Dzyaloshinskii–Moriya interaction can be nonzero. As the lattice distortion is not significant in the configuration with an O vacancy, we do not find strong canting.

2.2. Experimental

Figure 6 shows the XPS spectra of N, F co-substituted Cr_2O_3. In the N 1s spectrum of N, F co-substituted Cr_2O_3 we obtain only a single contribution at 399.5 eV, corresponding to the Cr–N bonds, whereas the F 1s spectrum can be deconvoluted into three contributions at 685.0, 686.5, and 688.1 eV. Taking the contribution from the highest binding energy for Cr–F bonds as substitutional fluorine,[3,4] the composition of N, F co-substituted Cr_2O_3 was calculated to be $Cr_2O_{2.79}N_{0.12}F_{0.09}$.

Cr_2O_3 has the corundum structure and doping with nitrogen and fluorine, even up to 10%, does not change the structure. Co-substitution of nitrogen and fluorine also does not change the structure and only results in minor changes in the lattice parameters. The experimental cell parameters of these compounds obtained from the Le Bail fitting (Figure S2) are $a=$ 4.9594 Å and $c=$13.5959 Å for undoped Cr_2O_3 and $a=$ 4.9419 Å and $c=$13.5734 Å for N, F co-substituted Cr_2O_3. Electronic absorption spectra show that the long-wavelength visible band extends to slightly longer wavelengths in N, F co-substituted Cr_2O_3 compared to pure Cr_2O_3.

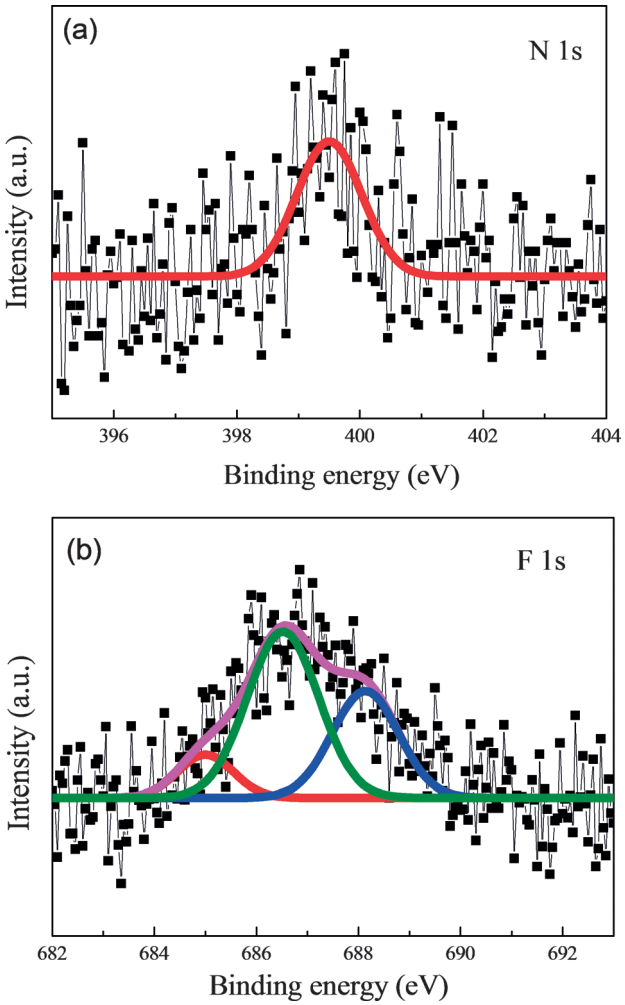

Figure 6. Core-level XPS spectra of a) N 1s and b) F 1s for N, F co-substituted Cr_2O_3

Undoped Cr_2O_3 shows a paramagnetic-to-collinear antiferromagnetic transition near 310 K. Below this temperature, as shown in Figure 7a, the moment decreases in field-cooled (FC) conditions (1000 Oe) until 200 K, but increases again as the temperature is decreased further. In the case of N, F co-substituted Cr_2O_3, we do not observe the paramagnetic-to-antiferromagnetic transition at 308 K, and a canted antiferromagnetic behavior is seen at approximately 285 K, below which the magnetization increases with decreasing temperature. At 1000 Oe and 10 K, we obtain the magnetization value of 0.0016 μ_B per Cr_2O_3 unit, owing to canting. The fluorine-doped sample also shows spin-canted behavior, with the value of magnetization amounting to 0.0018 μ_B per Cr_2O_3 unit at 1000 Oe. Magnetization versus field data (Figure 8) for N, F co-substituted Cr_2O_3 shows a typical hysteresis loop of a canted antiferromagnetic material with a coercive field (H_C) of 1.2 kOe at 2 K.[19–21] For the fluorine-doped sample H_C is found to be 1.4 kOe, whereas H_C in the case of undoped Cr_2O_3 is only 0.35 kOe. The relatively small values of magnetization per for-

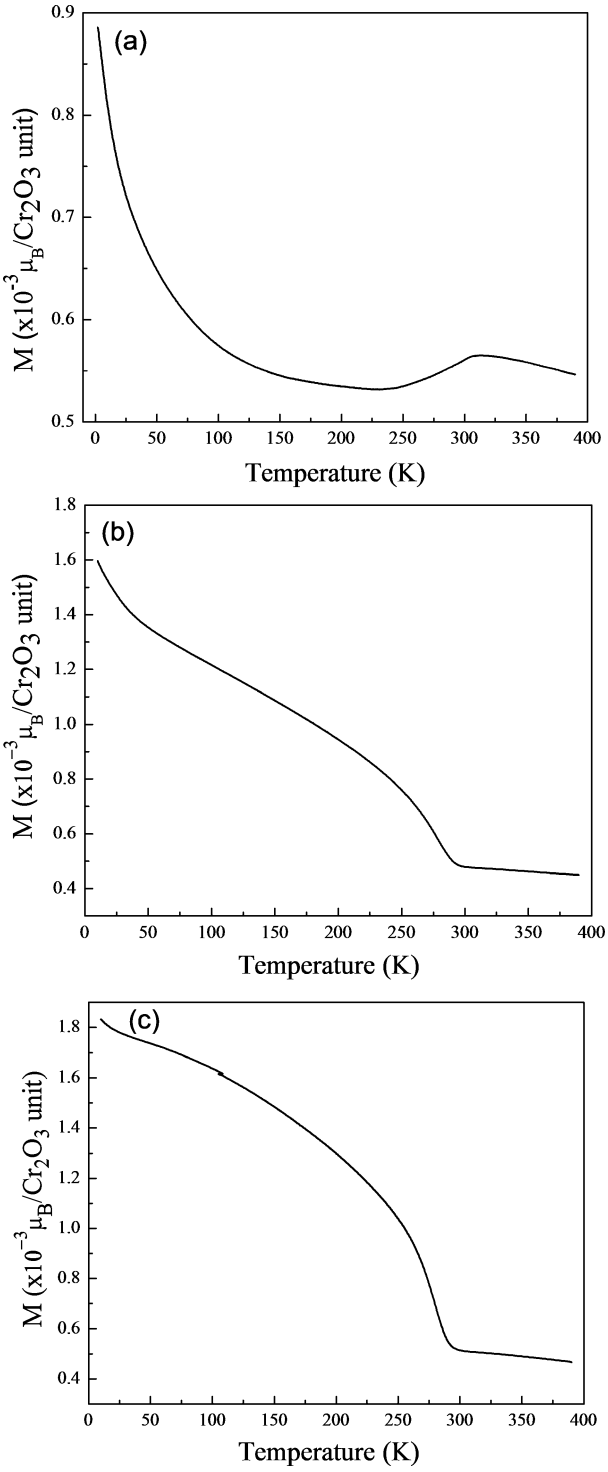

Figure 7. Field-cooled magnetization of a) undoped Cr_2O_3, b) N, F co-substituted Cr_2O_3, and c) F-doped Cr_2O_3 at 1000 Oe.

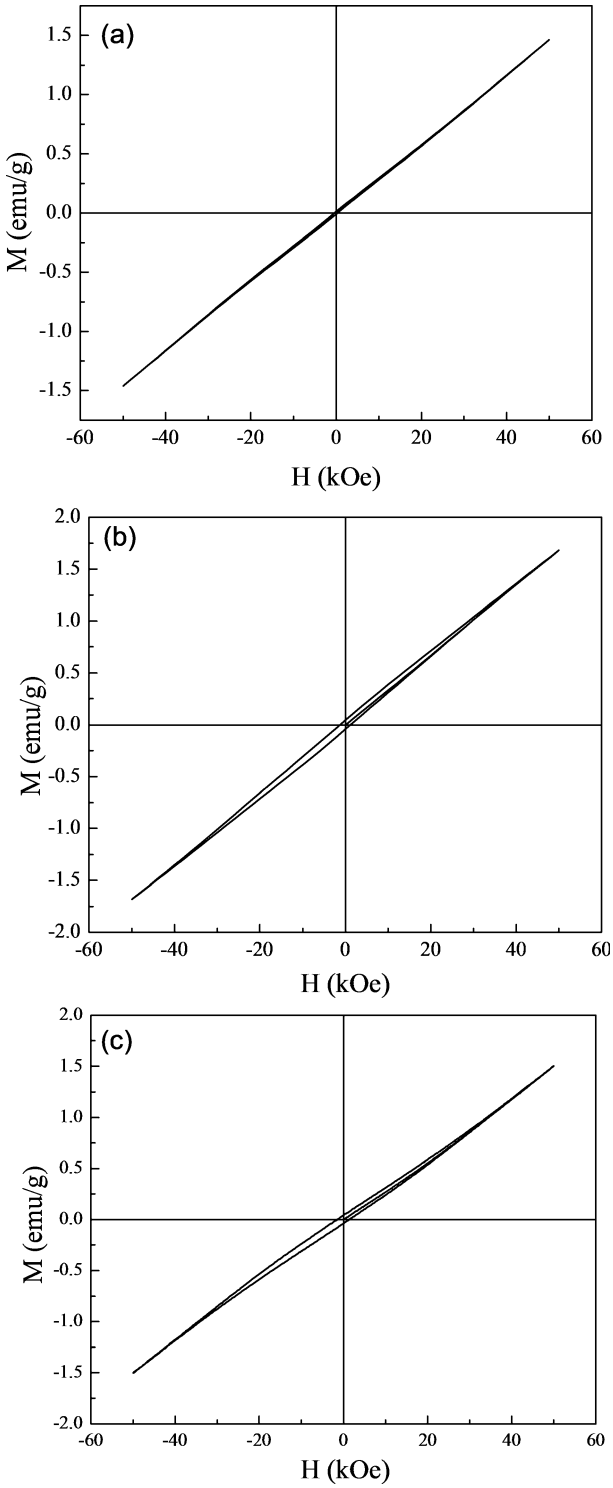

Figure 8. Low-temperature isothermal magnetization of a) undoped Cr_2O_3, b) N, F co-substituted Cr_2O_3, and c) F-doped Cr_2O_3 at 2 K.

mula unit and non-saturation of hysteresis loops even at high applied magnetic fields indicate that N, F co-substituted Cr_2O_3 and F-substituted Cr_2O_3 are canted antiferromagnetically and are not quite ferrimagnetic.

3. Conclusions

Our first-principles theoretical analysis shows that N substitution gives rise to the formation of a strong Cr–N bond and emergence of the N 2p sub-band at the top of the valence band. The d–d band gap of Cr_2O_3 is reduced by about 0.6 eV to a p–d gap with N and F co-substitution. The local spins in

N, F co-substituted Cr_2O_3 are canted, owing to the SOC that acts along with local structural distortion through the Dzyaloshinskii–Moriya interaction. Hole-mediated exchange and SOC are responsible for the magnetic behavior of N, F co-substituted Cr_2O_3. Experimentally, we observe canted antiferromagnetic behavior in both F-substituted and N, F co-substituted Cr_2O_3.

Computational Details

Our first-principles calculations are based on DFT with exchange-correction energy treated within a local density approximation (LDA), as implemented with projected augmented-wave (PAW)[22,23] potential in the Vienna ab initio simulation package (VASP).[24,25] We used a hexagonal periodic supercell cell containing 30 atoms (six formula units) to simulate pure and anion-substituted Cr_2O_3 (Figure 1a). In the simulation of the substitution with N or F alone, and for introducing an O vacancy, a random oxygen site in the supercell was picked. For co-substitution of N and F at oxygen sites in Cr_2O_3, we considered all possible combinations of pairs of oxygen sites to be substituted with one N and one F, respectively. This large number of configurations (288) was reduced, using the SOD[26] technique, to ten symmetry-inequivalent configurations. A plane-wave basis employed in representation of wavefunctions was truncated with an energy cutoff of 600 eV. The Brillouin zone integrations were sampled on $6\times6\times2$ uniform mesh of *k*-points by carrying out structural relaxation through energy minimization, and the density of states was calculated by using a $12\times12\times4$ uniform mesh of *k*-points. In addition to an accurate description of crystal field and exchange splitting, electron correlations associated with a partially filled Cr 3d orbital were included through use of spherically averaged on-site correlations with the Hubbard *U–J* correction[27] ($U=4.00$ eV, $J=0.58$ eV[13]). In calculations of non-collinearly ordered magnetic structures, we used 1) the FU method with simultaneous relaxation of atomic structure and magnetic ordering and 2) self-consistent calculations[17] with SOC, which measure the interaction of orbital degree of freedom with magnetic spin.[28]

Experimental Section

For the synthesis of Cr_2O_3 co-substituted with N and F, $Cr(NO_3)_3.6H_2O$ (10 g) was dissolved in water (220 mL), and an excess of aqueous ammonium hydroxide was added to it. The mixture was stirred for 1 h followed by centrifugation and washing with deionized water. The solid powder was dried in oven at 80 °C for 10 h. The dried powder was mixed and ground with excess NH_4F (20 times excess in molar equivalents). The mixture was placed in an alumina boat and heated in a tube furnace in flowing ammonia at 700 °C for 4 h. For fluorine doping alone, the mixture was heated under the similar conditions, but in a nitrogen flow. Nitrogen doping of Cr_2O_3 was found to be difficult, owing to the formation of CrN impurities.

X-ray diffraction patterns were recorded in a Bruker D8 Discover diffractometer and Rigaku-99 diffractometer by using CuKα radiation. To obtain cell parameters of the doped and undoped Cr_2O_3 powders, Le Bail fitting was carried out using Fullprof software.[29] XPS spectra were recorded in an Omicron Nanotechnology Spectrometer with MgKα as the X-ray source. Magnetic measurements were carried out by using SQUID VSM (Quantum Design, USA).

Keywords: anion substitution · chromium oxide · density functional calculations · magnetic properties · spin canting

[1] A. Sundaresan, R. Bhargavi, N. Rangarajan, U. Siddesh, C. N. R. Rao, *Phys. Rev. B* **2006**, *74*, 161306.
[2] A. Sundaresan, C. N. R. Rao, *Nano Today* **2009**, *4*, 96–106.
[3] R. Saha, S. Revoju, V. I. Hegde, U. V. Waghmare, A. Sundaresan, C. N. R. Rao, *ChemPhysChem* **2013**, *14*, 2672–2677.
[4] N. Kumar, U. Maitra, V. I. Hegde, U. V. Waghmare, A. Sundaresan, C. N. R. Rao, *Inorg. Chem.* **2013**, *52*, 10512–10519.
[5] A. Iyama, T. Kimura, *Phys. Rev. B* **2013**, *87*, 180408.
[6] S. Sahoo, C. Binek, *Philos. Mag. Lett.* **2007**, *87*, 259–268.
[7] L. W. Finger, R. M. Hazen, *J. Appl. Phys.* **1980**, *51*, 5362–5367.
[8] P. J. Brown, J. B. Forsyth, E. Lelievre-Berna, F. Tasset, *J. Phys. Condens. Matter* **2002**, *14*, 1957.
[9] L. M. Corliss, J. M. Hastings, R. Nathans, G. Shirane, *J. Appl. Phys.* **1965**, *36*, 1099–1100.
[10] S. Foner, *Phys. Rev.* **1963**, *130*, 183–197.
[11] J. A. Crawford, R. W. Vest, *J. Appl. Phys.* **1964**, *35*, 2413–2418.
[12] J. Zaanen, G. A. Sawatzky, J. W. Allen, *Phys. Rev. Lett.* **1985**, *55*, 418–421.
[13] S. Shi, A. L. Wysocki, K. D. Belashchenko, *Phys. Rev. B* **2009**, *79*, 104404.
[14] D. Li, Z. Han, J. G. Zheng, X. L. Wang, D. Y. Geng, J. Li, Z. D. Zhang, *J. Appl. Phys.* **2009**, *106*, 053913–053913–5.
[15] A. Rohrbach, J. Hafner, G. Kresse, *Phys. Rev. B* **2004**, *70*, 125426.
[16] N. Kumar, J. Pan, N. Aysha, U. V. Waghmare, A. Sundaresan, C. N. R. Rao, *J. Phys. Condens. Matter* **2013**, *25*, 345901.
[17] D. Hobbs, G. Kresse, J. Hafner, *Phys. Rev. B* **2000**, *62*, 11556–11570.
[18] I. A. Sergienko, E. Dagotto, *Phys. Rev. B* **2006**, *73*, 094434.
[19] D. Jagadeesan, U. Mansoori, P. Mandal, A. Sundaresan, M. Eswaramoorthy, *Angew. Chem. Int. Ed.* **2008**, *120*, 7799–7802; *Angew. Chem.* **2008**, *120*, 7799–7802.
[20] L. Liu, H.-Z. Kou, W. Mo, H. Liu, Y. Wang, *J. Phys. Chem. B* **2006**, *110*, 15218–15223.
[21] S. Mitra, S. Das, K. Mandal, S. Chaudhuri, *Nanotechnology* **2007**, *18*, 275608.
[22] P. E. Blöchl, *Phys. Rev. B* **1994**, *50*, 17953–17979.
[23] G. Kresse, D. Joubert, *Phys. Rev. B* **1999**, *59*, 1758–1775.
[24] G. Kresse, J. Hafner, *Phys. Rev. B* **1993**, *48*, 13115–13118.
[25] G. Kresse, J. Furthmüller, *Phys. Rev. B* **1996**, *54*, 11169–11186.
[26] R. Grau-Crespo, S. Hamad, C. R. A. Catlow, N. H. De Leeuw, *J. Phys. Condens. Matter* **2007**, *19*, 256201.
[27] S. L. Dudarev, G. A. Botton, S. Y. Savrasov, C. J. Humphreys, A. P. Sutton, *Phys. Rev. B* **1998**, *57*, 1505–1509.
[28] H. J. Gotsis, N. Kioussis, D. A. Papaconstantopoulos, *Phys. Rev. B* **2006**, *73*, 014436.
[29] J. Rodríguez-Carvajal, *Physica B* **1993**, *192*, 55–69.

Received: November 19, 2014
Published online on ■■ ■■, 2015

*J. Pan, U. V. Waghmare, N. Kumar, C. O. Ehi-Eromosele, C. N. R. Rao**

■■ – ■■

Effect of Nitrogen and Fluorine Co-substitution on the Structure and Magnetic Properties of Cr_2O_3

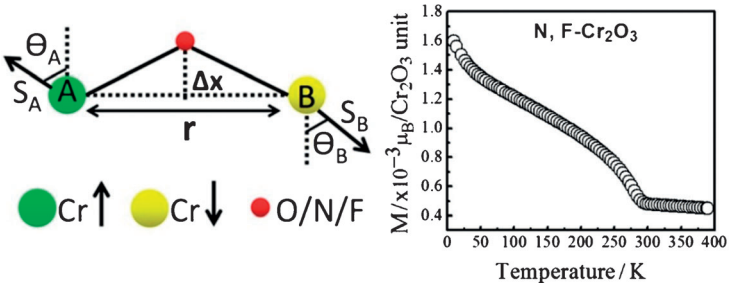

Don't be DFT: Spin–orbit coupling along with local structural distortion gives rise to strong spin canting in N, F co-substituted Cr_2O_3.